Tie-dyed2 Encodes a Callose Synthase That Functions in Vein Development and Affects Symplastic Trafficking within the Phloem of Maize Leaves[1,2][C][W][OA]

Thomas L. Slewinski, R. Frank Baker, Adam Stubert, and David M. Braun*

Department of Plant Biology, Cornell University, Ithaca, New York 14853 (T.L.S.); Division of Biological Sciences and Interdisciplinary Plant Group, Missouri Maize Center, University of Missouri, Columbia, Missouri 65211 (R.F.B., D.M.B.); and Department of Biology, Pennsylvania State University, University Park, Pennsylvania 16802 (A.S.)

The *tie-dyed2* (*tdy2*) mutant of maize (*Zea mays*) displays variegated green and yellow leaves. Intriguingly, the yellow leaf tissues hyperaccumulate starch and sucrose, the soluble sugar transported long distance through the phloem of veins. To determine the molecular basis for *Tdy2* function, we cloned the gene and found that *Tdy2* encodes a callose synthase. RNA in situ hybridizations revealed that in developing leaves, *Tdy2* was most highly expressed in the vascular tissue. Comparative expression analysis with the vascular marker maize *PINFORMED1a*-yellow fluorescent protein confirmed that *Tdy2* was expressed in developing vein tissues. To ascertain whether the defect in *tdy2* leaves affected the movement of sucrose into the phloem or its long-distance transport, we performed radiolabeled and fluorescent dye tracer assays. The results showed that *tdy2* yellow leaf regions were defective in phloem export but competent in long-distance transport. Furthermore, transmission electron microscopy of *tdy2* yellow leaf regions showed incomplete vascular differentiation and implicated a defect in cell-to-cell solute movement between phloem companion cells and sieve elements. The disruption of sucrose movement in the phloem in *tdy2* mutants provides evidence that the *Tdy2* callose synthase functions in vascular maturation and that the vascular defects result in impaired symplastic trafficking into the phloem translocation stream.

The maize (*Zea mays*) leaf is organized into repetitive parallel units centered around veins (Esau, 1943; Evert et al., 1978). The veins exhibit Kranz anatomy: an outer ring of photosynthetic mesophyll (M) cells encircle a ring of photosynthetic bundle-sheath (BS) cells, which in turn encircle the vein (Esau, 1977). Each vein contains two tissues: (1) the water-transporting tissue, the xylem, comprising xylem elements and xylem parenchyma cells; and (2) the photoassimilate-transporting tissue, the phloem, comprising sieve elements (SEs), companion cells (CCs), and vascular parenchyma (VP) cells (Esau, 1977). Three classes of longitudinally oriented veins are present in the maize leaf (Russell and Evert, 1985). The large vein class contains large metaxylem vessels and primarily functions in long-distance assimilate transport (Fritz et al., 1989). The intermediate and small veins lack large metaxylem vessels and principally function to load Suc into the phloem (Fritz et al., 1983).

C_4 carbon assimilation in maize results in Suc production in the M cells (Lunn and Furbank, 1999). The subsequent export of Suc from the leaf (source tissue) to the nonphotosynthetic (sink) tissues requires its transit through a number of cell types and tissues. Initially, Suc moves from the M cells into the BS cells and then into the VP cells via the abundant plasmodesmata (PD) present at each cellular interface (Fig. 1A; Evert et al., 1978; Braun and Slewinski, 2009). This diffusion from cell to cell through the PD is referred to as symplastic transport (Roberts and Oparka, 2003). After entering the VP cells, Suc is exported to the apoplast, the cell wall space proximal to the CC and SE, likely by SWEET proteins (Baker et al., 2012; Braun, 2012; Chen et al., 2012). The CC and SE are connected by abundant PD but display very limited connection to other surrounding cell types (Evert et al., 1978). To load Suc into the CC-SE complexes, Suc transporter (SUT) proteins located on the plasma membrane actively pump Suc from the apoplastic space into the

[1] This work was supported by the National Research Initiative and Agriculture and Food Research Initiative Competitive Grants Program from the U.S. Department of Agriculture National Institute of Food and Agriculture (grant no. 2008–35304–30063) and by the National Science Foundation Plant Genome Research Program (grant no. IOS–1025976 to D.M.B.).

[2] This paper is dedicated to Stanley E. Mills (1922–2011), mentor to D.M.B., whose creativity, curiosity, and tenacity remain an inspiration.

* Corresponding author; e-mail braundm@missouri.edu.

The author responsible for distribution of materials integral to the findings presented in this article in accordance with the policy described in the Instructions for Authors (www.plantphysiol.org) is: David M. Braun (braundm@missouri.edu).

[C] Some figures in this article are displayed in color online but in black and white in the print edition.

[W] The online version of this article contains Web-only data.

[OA] Open Access articles can be viewed online without a subscription.

www.plantphysiol.org/cgi/doi/10.1104/pp.112.202473

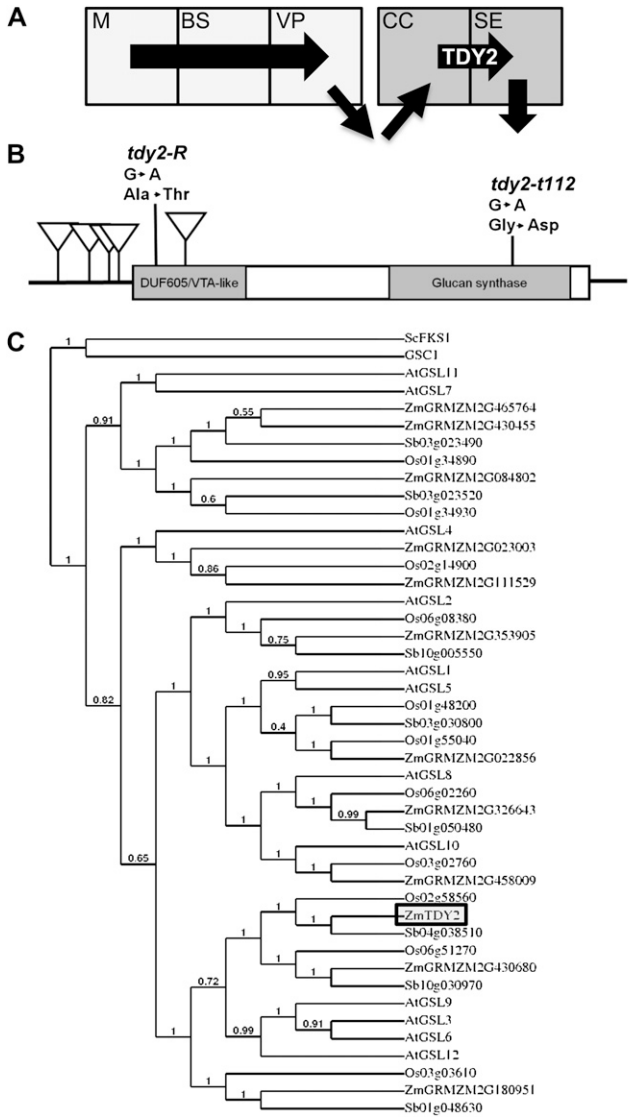

Figure 1. *Tdy2* cloning and phylogenetic analysis. A, Simplified path of Suc movement in a maize leaf (arrows). Suc is synthesized in M cells, moves into BS cells, and then into VP cells through PD. Suc is exported to the apoplast and then imported into the CC. Suc moves through the PD into the SE and then into the adjoining SE (downward arrow). TDY2 promotes Suc trafficking through the CC-SE PD. B, Schematic of the *Tdy2* mRNA showing the location of seven identified mutant alleles. *Mu* transposon insertions are represented as downward triangles. Mutations in two EMS-derived alleles, *tdy2-R* and *tdy2-t112*, and the resulting amino acid changes are also shown. Boxes indicate protein-coding regions, and lines represent the 5′ and 3′ UTRs. Shaded boxes indicate conserved domains in the protein sequence. C, Neighbor-joining phylogenetic analysis of full-length callose synthase proteins. At, Arabidopsis; Os, rice; Sb, sorghum, Zm, maize. Numbers on the tree branches indicate support values as a fraction of 1. The β-1,3-glucan synthases GSC1 (XP_721429) from *Candida albicans* and ScFKS1 (EEU05506) from *Saccharomyces cerevisiae* were used as outgroups.

cytosol (Lalonde et al., 2004; Sauer, 2007; Braun and Slewinski, 2009; Kühn and Grof, 2010; Slewinski and Braun, 2010a; Ainsworth and Bush, 2011; Ayre, 2011). The resultant concentrated Suc then moves symplastically into the SE through the abundant PD. In response to the increased sugar concentration within the phloem, water enters the phloem via osmosis from the xylem. Suc then moves from source to sink tissues by means of osmotically generated pressure flow within the interconnected SE (Lalonde et al., 2003).

Genetic screens for mutants that hyperaccumulate carbohydrates in their leaves could be used to identify genes functioning in any of the above steps, including Suc export from the phloem, symplastic transport, starch catabolism in the photosynthetic cells, and phloem development (Russin et al., 1996; Blauth et al., 2001; Dinges et al., 2003; Braun et al., 2006; Baker and Braun, 2008; Slewinski et al., 2009; Slewinski and Braun, 2010b). In maize, loss-of-function mutations in the *Sut1* gene confer a strong carbohydrate hyperaccumulation phenotype in leaves (Slewinski et al., 2009, 2010). The mutants are severely impeded in loading Suc into the phloem, which results in high concentrations of Suc, Glc, Fru, and starch in leaves and to premature leaf senescence. Similar phenotypes have been reported for mutations in the principal SUT responsible for Suc phloem loading in other apoplastic loading species (Riesmeier et al., 1994; Kühn et al., 1997; Bürkle et al., 1998; Gottwald et al., 2000; Hackel et al., 2006; Srivastava et al., 2008). Interestingly, in addition to increased starch and soluble sugars in leaves, potato (*Solanum tuberosum*) plants lacking the SUT1 protein due to antisense RNA expression accumulated excess fixed carbon as oil droplets (Schulz et al., 1998). Plants mutant for another gene, *Sucrose export defective1* (*Sxd1*), develop yellow leaf regions that initiate at the leaf tip and progressively spread down the leaf (Russin et al., 1996; Provencher et al., 2001). Moreover, the yellow leaf regions contain greatly elevated levels of starch and soluble sugars. Within these yellow regions, the PD between the BS-VP cells are occluded with ectopic callose, which prevents Suc movement into the veins (Botha et al., 2000). Intriguingly, *Sxd1* encodes an enzyme in the vitamin E biosynthetic pathway (Sattler et al., 2003). The *sxd1* mutant defect is consistent with the possibility that different mechanisms could lead directly or indirectly to a carbon accumulation phenotype.

Two additional maize mutants, *tie-dyed1* (*tdy1*) and *tdy2*, condition a nonclonal pattern of yellow and green regions in the leaves (Braun et al., 2006; Baker and Braun, 2007, 2008). Similar to *sxd1* mutants, the yellow leaf tissues in the *tdy* mutants hyperaccumulate starch and soluble sugars, whereas the green tissues are indistinguishable from the wild type. The *tdy* yellow and green regions form during the emergence of the leaf from the whorl; however, in contrast to the *sxd1* leaf phenotype, which becomes increasingly severe, the yellow and green regions in *tdy* mutants are developmentally stable throughout the life of the leaf. Previous evidence suggested that the *Tdy* pathway functions independently of both *Sxd1* and starch metabolism, indicating that the *Tdy* genes define a distinct

genetic pathway (Baker and Braun, 2008; Ma et al., 2008; Slewinski et al., 2008). *Tdy1* encodes a novel gene specifically expressed in the phloem (Ma et al., 2009). To determine the molecular function of *Tdy2*, we cloned the gene and characterized its expression pattern using reverse transcription (RT)-PCR and RNA in situ hybridization. Radioactive and fluorescent dye tracer studies, as well as ultrastructural studies using transmission electron microscopy (TEM), indicated that *tdy2* mutants have defects in the functional development of the phloem and that these defects block cell-to-cell symplastic movement through PD from phloem CC to SE.

RESULTS

Tdy2 Encodes a Callose Synthase

To understand the molecular function of *Tdy2*, we cloned the gene using a combination of map-based cloning and *Mutator* (*Mu*) transposon-tagging strategies. The *tdy2-Reference* (*tdy2-R*) locus was fine-mapped to the long arm of chromosome 5, between a single nucleotide polymorphism marker in an oligopeptidase gene and the telomere. We fine-mapped the region containing the *Tdy2* gene to 10 bacterial artificial chromosomes containing approximately 35 genes. Because of suppressed recombination in this chromosomal region, a sequence-independent approach was used to identify candidate genes. Using adaptor-ligated thermal asymmetric interlaced (TAIL)-PCR (Singer and Burke, 2003), flanking genomic DNA was amplified from a cosegregating *Mu* insertion in the *tdy2-m248* allele and sequenced (Table I; Supplemental Materials and Methods S1). We determined that the *Mu* element had inserted into the 5′ untranslated region (UTR) of a callose synthase, one of the genes identified within the mapping interval. Analysis of multiple, independently derived alleles verified that we cloned the correct gene (Fig. 1B; Table I). RT-PCR analysis on RNA isolated from the leaves of plants homozygous for the *tdy2-m165* allele, which contains a *Mu* insertion within the *Tdy2* protein-coding region (Table I), detected a chimeric RNA molecule containing part of the transposable element and missing the 3′ end of the *Tdy2* transcript, which encodes functionally important residues of the enzyme catalytic domain and suggests that this is likely a null allele (Supplemental Fig. S1; Verma and Hong, 2001). Similar to Arabidopsis (*Arabidopsis thaliana*) T-DNA insertion mutations in most callose synthase genes (Enns et al., 2005), no phenotype was observed in plants homozygous for the *tdy2-Mu* insertion alleles (Fig. 2; Supplemental Fig. S1), suggesting genetic redundancy. However, heteroallelic plants carrying both a *tdy2-Mu* transposable element insertion allele and the *tdy2-R* allele had leaves with mild yellow regions that hyperaccumulated starch (Fig. 2). These data are consistent with our previous gene dosage analysis of *tdy2-R*, which suggested that it retains some function and is not a null allele (Baker and Braun, 2008). Interestingly, the *tdy2-R* and *tdy2-t112* alleles result from missense mutations and are the only two alleles to confer visible phenotypes as homozygotes, suggesting that they encode defective proteins that interfere with normal TDY2 function (for discussion, see Baker and Braun, 2008).

Callose synthases, also known as glucan synthase-like genes (GSLs), synthesize callose, a β-1,3-linked polymer of Glc (Verma and Hong, 2001). Callose is deposited at various times and locations in plants, such as during new cell wall formation, in response to wounding, in growing pollen tubes, at sieve plates, and around the neck regions of PD (Chen and Kim, 2009). Phylogenetic analysis revealed the callose synthase encoded by *Tdy2* has an ortholog in rice (*Oryza sativa*) and sorghum (*Sorghum bicolor*) and a paralog in maize that is present in both rice and sorghum (Fig. 1C), consistent with the ancient whole-genome duplication at the origin of the grasses (Jiao et al., 2011). TDY2 is co-orthologous to a subfamily of Arabidopsis callose synthases consisting of AtGSL3, AtGSL6, AtGSL9, and AtGSL12 (Enns et al., 2005; Chen and Kim, 2009; Vatén et al., 2011).

Table I. *Molecular characterization of tdy2 mutant alleles*

Allele	Mutation	Position
tdy2-R	GCC → ACC	163 in mRNA
	Ala → Thr	55 in protein
tdy2-t112	GGT → GAT	4,481 in mRNA
	Gly → Asp	1,494 in protein
tdy2-Mu103	*Mu8* insertion	5′ UTR, −289 bp from ATG
tdy2-Mu165	*Mu1* insertion	Exon 1, +223 bp from ATG
tdy2-Mu199	*Mu1* insertion	5′ UTR, −254 bp from ATG
tdy2-Mu248	*Mu1* insertion	5′ UTR, −222 bp from ATG
tdy2-Mu385	*Mu1* insertion	5′ UTR, −226 bp from ATG

Tdy2 Expression

To determine in which tissues *Tdy2* is expressed, we conducted RT-PCR on RNA isolated from wild-type B73 tissues. *Tdy2* transcripts were present in all tissues analyzed, including mature source and immature sink leaves, roots, developing tassels, and ears (Fig. 3A). To examine the cell-specific expression of *Tdy2*, we performed RNA in situ hybridizations on developing leaves (Fig. 3, B, D, and F). *Tdy2* mRNA was expressed at low levels in all cells; however, the expression was much greater in developing veins. In the youngest developing leaves adjacent to the shoot apex, a thin strip of expression was observed in the leaf center, which corresponds to the procambium (Fig. 3B; Esau, 1943). In slightly older leaves, *Tdy2* expression was visible as punctate staining in the developing phloem and xylem (Fig. 3, D and F). The RNA sense-strand control showed no signal (Fig. 3G).

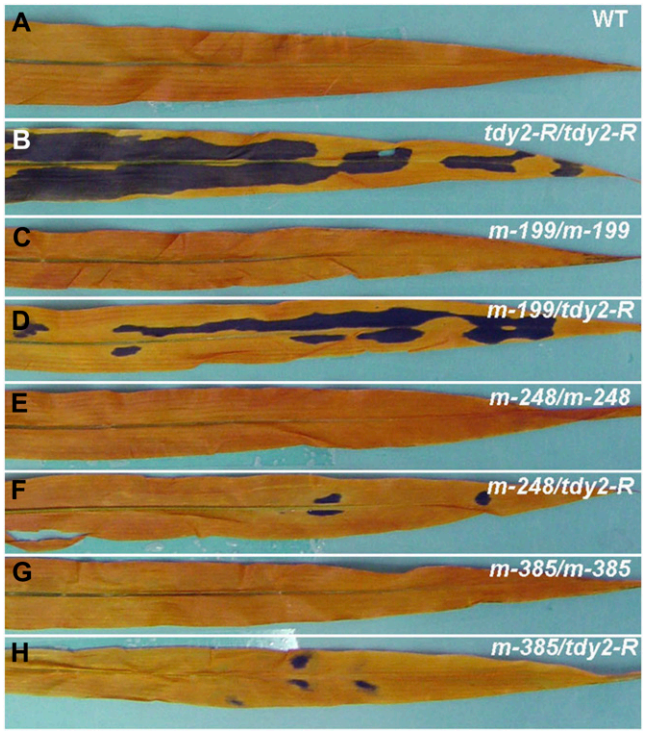

Figure 2. Alleles containing *Mu* insertions in *Tdy2* do not condition a phenotype as homozygotes. Only when insertion alleles are heteroallelic with the *tdy2-R* allele do plants display a mild starch accumulation phenotype. Leaves cleared of photosynthetic pigments and stained for starch (dark brown pigmentation) are shown. A, The wild type (WT). B, *tdy2-R* homozygous mutant. C, *tdy2-m199* homozygous plant. D, *tdy2-m199/tdy2-R* heteroalleleic combination. E, *tdy2-m248* homozygous plant. F, *tdy2-m248/tdy2-R* heteroallelic combination. G, *tdy2-m385* homozygous plant. H, *tdy2-m385/tdy2-R* heteroallelic combination. [See online article for color version of this figure.]

To examine further the developmental timing of *Tdy2* expression, we compared it with a marker for early vascular development in maize, PINFORMED1a (ZmPIN1a)-YFP (for yellow fluorescent protein; Gallavotti et al., 2008). ZmPIN1a is co-orthologous to the Arabidopsis *PIN1* gene, which encodes a polar auxin transporter that functions in vein development (Wenzel et al., 2007). Mirroring the expression of *Tdy2*, ZmPIN1a expression was initially observed as a stripe of procambium in initiating leaf primordia and later in punctate regions in the developing lateral veins (Fig. 3, C and E). These data demonstrate that *Tdy2* is expressed most strongly in developing veins.

Phloem Export and Transport in *tdy2* Mutants

From previous work, we inferred that *tdy2* mutants are defective in Suc export from leaves (Baker and Braun, 2008). To test this hypothesis, we monitored the movement of ^{14}C-labeled Suc applied to mutant and wild-type leaves. When ^{14}C-labeled Suc was applied to the abraded surface near the tip of a wild-type mature leaf (Fig. 4A), it entered into the leaf apoplast, was loaded into the phloem, and was transported within the SE toward the leaf base (Fig. 4B). However, when the labeled Suc was applied to *tdy2* mutant yellow leaf tissue (Fig. 4C), it did not move beyond the site of application (Fig. 4D). To determine whether the impaired Suc movement resulted from a disruption in phloem export or long-distance transport, we applied ^{14}C-labeled Suc to *tdy2* mutant green tissue near the tip of a leaf that had yellow tissues near its base (Fig. 4E). In the *tdy2* green leaf tissue, the labeled Suc was loaded into and transported through the phloem in a manner similar to that in the wild type (Fig. 4F). Significantly, after entering the phloem translocation stream, the labeled Suc was translocated through the *tdy2* yellow leaf tissues, indicating that long-distance phloem transport was not disrupted. Hence, these results show that the export of Suc into the phloem of *tdy2* mutant yellow leaf regions was impaired.

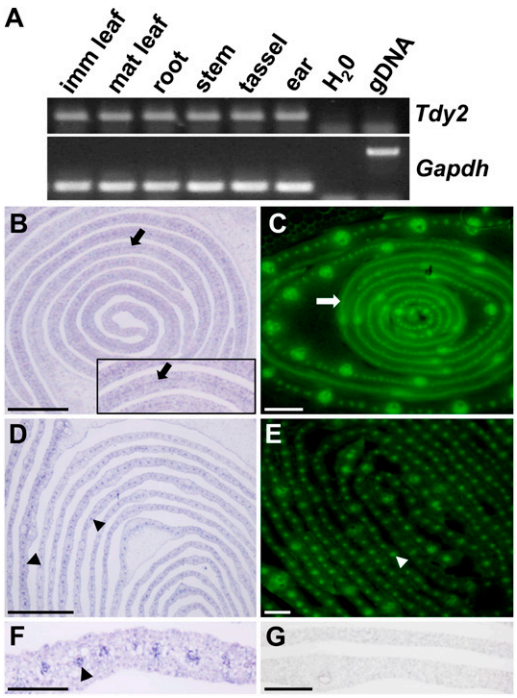

Figure 3. *Tdy2* and *ZmPIN1a*-YFP expression. A, *Tdy2* RT-PCR in different tissue samples showing broad expression of the *Tdy2* gene. imm, Immature; mat, mature; H_2O, no-template control; gDNA, genomic DNA control; *Gapdh*, *glyceraldehyde-3-phosphate-dehydrogenase*, shown as a complementary DNA normalization control. B, D, and F, *Tdy2* RNA in situ hybridization analysis on wild-type B73 developing leaf tissue using the antisense probe. Arrows show the procambial strand; arrowheads indicate developing veins. The inset in B shows a closeup view. C and E, ZmPIN1a-YFP expression in developing leaves of similar age as shown in B and D, illuminating the procambium and developing veins. B and C show young leaves close to the apex, and D to G show slightly older leaves. G, *Tdy2* sense-strand control RNA in situ hybridization. Bars = 100 μm in B to E and 25 μm in F and G. [See online article for color version of this figure.]

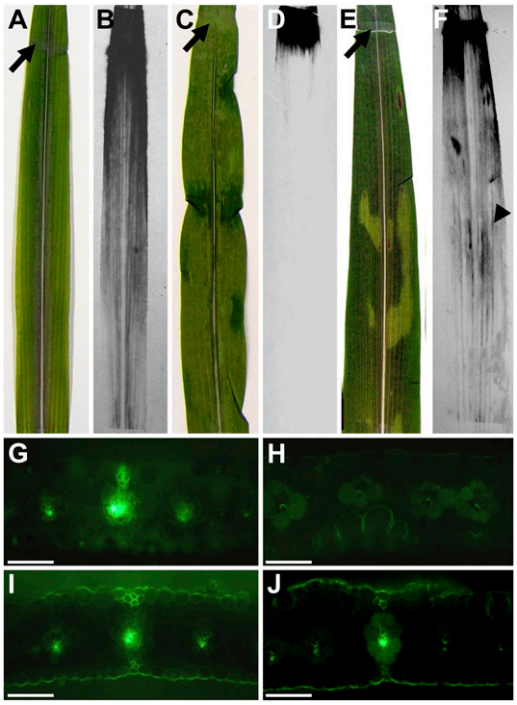

Figure 4. ^{14}C-labeled Suc and CF transport in wild-type and *tdy2* mutant leaves. A, C, and E, Black arrows indicate sites of abrasion and application of [^{14}C]Suc to leaves. B, D, and F, Autoradiographs showing [^{14}C]Suc localization in leaves 1 h after application. A and B, Wild-type leaf showing normal phloem loading and transport of [^{14}C]Suc. C and D, A mostly yellow *tdy2* mutant leaf in which ^{14}C-labeled Suc was applied to a yellow region, showing that labeled Suc did not move from the site of application. E and F, *tdy2* mutant leaf in which labeled Suc was applied to green tissue distal to the yellow tissue, showing that labeled Suc was loaded, translocated long distance in the phloem, and passed through the phloem in the yellow tissue (arrowhead). G to J, CF transport assays in which CFDA was applied to the leaf tissue near the tip; cross-sections were taken 5 to 7 cm proximal to the application site. Bright green fluorescence shows the presence of CF in the phloem. G, Wild-type leaf showing normal phloem translocation. H, A mostly yellow *tdy2* mutant leaf in which CFDA was applied to distal yellow tissue; a cross section was taken from a proximal yellow region, showing that CF was not able to be translocated through the phloem. I, *tdy2* mutant in which CFDA was applied to distal green tissue; a cross-section was taken from proximal green tissue, showing normal phloem translocation. J, *tdy2* mutant tissue in which CFDA was applied to distal green tissue; a cross-section was taken from proximal yellow tissue, which shows that CF can enter the phloem translocation stream in the green tissue and subsequently be translocated through yellow tissues, indicating that long-distance phloem transport is unobstructed. Bars = 100 μm. [See online article for color version of this figure.]

To independently verify these results, we performed carboxyfluorescein-diacetate (CFDA) labeling, an assay routinely used to monitor phloem transport (Wright and Oparka, 1996; Ma et al., 2009; Zhang et al., 2010). CFDA is an uncharged, nonfluorescent molecule and is able to passively cross cell membranes. Esterases present in the cytoplasm remove the diacetate groups, converting the molecule to carboxyfluorescein (CF), a fluorescent, polar compound that is detectable as a symplastic tracer (Wright and Oparka, 1996). In wild-type tissues, CFDA entered into the phloem and CF was transported through it (Fig. 4G). However, CF failed to be transported through the phloem when CFDA was applied to *tdy2* yellow leaf tissues (Fig. 4H). By contrast, CFDA that was applied to *tdy2* mutant green leaf regions located distal to yellow regions entered the phloem, with CF subsequently translocated through both green and yellow tissues (Fig. 4, I and J). Together, the [^{14}C]Suc and CFDA labeling data indicate that the defect in the *tdy2* yellow leaf tissues is specifically a failure of solutes to enter the phloem translocation stream and not in their long-distance transport through the veins.

Ultrastructural Abnormalities in *tdy2* Mutant Vascular Cells

The [^{14}C]Suc and CFDA labeling studies showed that *tdy2* mutants were compromised in Suc phloem export, indicating that the defect was in the veins. Therefore, we examined the ultrastructure of the *tdy2* mutant veins for abnormalities. Defects were observed in both the xylem and phloem (Fig. 5).

During the development of wild-type veins, metaxylem vessels undergo programmed cell death, which requires autophagy of cellular contents (Turner et al., 2007). At maturity, the vessels are dead and have no cellular contents (Fig. 5, A and C; Esau, 1977). However, within the *tdy2* mutant yellow leaf regions, we observed that the metaxylem vessels sometimes contained starch granules and other cellular debris (Fig. 5, B, D, and E; Supplemental Fig. S3), a phenotype that, to our knowledge, has not been previously reported. In the most severe cases, the new xylem daughter cell contained abundant cellular contents, such as starch, mitochondria, and fragments of membrane-bound organelles. Hence, the cell failed to complete autolysis, suggesting that the cell death program was interrupted or arrested (Fig. 5, D and E; Supplemental Fig. S3). Additionally, in the wild-type xylem, the portion of the VP cell wall abutting the xylem element is modified and appears fibrous (Fig. 5F; Evert et al., 1978). This cellular interface has been proposed to facilitate the influx of water into the VP cell from the xylem (Botha et al., 2008). However, in the minor veins of *tdy2* yellow leaf tissue, no instances of a fibrous cell wall between the VP and xylem cells were ever observed (Fig. 5G). Instead, the primary cell wall remained homogenous in appearance around the cell periphery. By contrast, the fibrous cell wall was present at the VP-xylem element cell interface in the *tdy2* green leaf tissue (Supplemental Fig. S2). The defect in cell wall formation between the xylem vessel and the xylem VP cell, and the incomplete autolysis phenotype in *tdy2* yellow leaf tissues, are consistent with *Tdy2* vascular expression and function early during vein development.

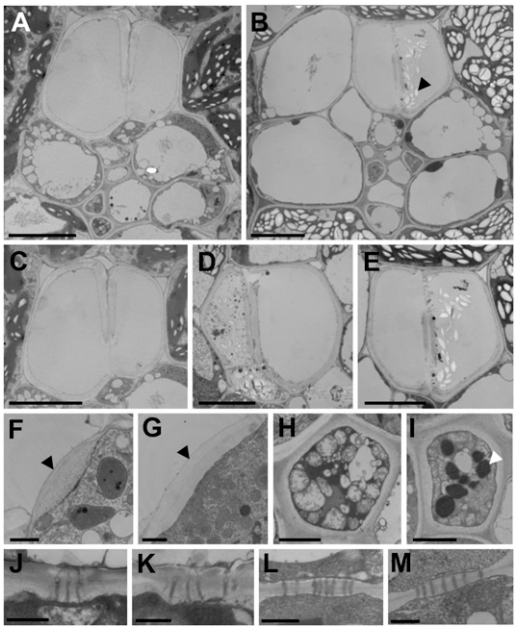

Figure 5. TEM images of small veins from mature leaves of wild-type and *tdy2* mutant yellow leaf tissues. A and B, Overview of small veins from wild-type (A) and *tdy2* mutant yellow leaf (B) tissues. C to E, Xylem elements in wild-type (C) and *tdy2* mutant (D and E) vein tissues. C and E are closeups of the xylem in A and B, respectively. Starch granules (black arrowhead in B) and cellular debris are evident in some *tdy2* xylem elements. F and G, Cell wall between VP and xylem element (black arrowheads) in the wild type (F) and the *tdy2* mutant (G). H and I, CC from the wild type (H) and the *tdy2* mutant (I). Oil droplets (white arrowhead) are unusually large and abundant in the CC of *tdy2* yellow leaf regions. J and K, PD between CC-SE in the wild type (J) and the *tdy2* mutant (K). L and M, PD between VP-VP cells in the wild type (L) and the *tdy2* mutant (M). Bars = 10 μm in A to E, 1 μm in F and G, 2 μm in H and I, and 0.5 μm in J to M.

TEM examinations of the phloem tissue in *tdy2* yellow leaf regions also identified structural perturbations. In wild-type phloem, CCs typically contain a high density of mitochondria, small vacuoles, and a dense cytoplasm containing small oil droplets (Fig. 5H; Evert et al., 1978). In the CC of the *tdy2* yellow leaf tissue, both the mitochondria and small vacuoles appeared similar to those of the wild type, but the frequency and size of the oil droplets were significantly increased (Fig. 5I). Because the oil droplets in the CC are composed of lipids (Schulz et al., 1998; Lersten et al., 2006), this finding indicates that *tdy2* mutant CCs contain high levels of carbon. In most cases, the SE in *tdy2* mutant leaves appeared normal, although in rare instances they contained remnant cellular contents (Supplemental Fig. S4). No ultrastructural alterations were identified in the veins of green tissue from *tdy2* mutant leaves (Supplemental Fig. S2). Therefore, these data indicate that within the *tdy2* yellow leaf regions, the CC accumulate an excessive amount of assimilated carbon and suggest that the transport blockage is located at the CC-SE interface.

PD Appear Unaffected in *tdy2* Veins

Suc movement from the CC into the SE occurs through PD. A possibility to explain the *tdy2* carbohydrate hyperaccumulation phenotype is that alterations in PD ultrastructure limit the symplastic movement of Suc between cells (Slewinski and Braun, 2010a). Previously, we used TEM to examine the PD along the symplastic path from the M to the VP cells but did not identify any structural defects (Baker and Braun, 2008). Because *Tdy2* is expressed most highly in the developing veins, we inspected the PD between vascular cells in leaf veins. Despite an extensive examination of hundreds of PD located at all cellular interfaces in veins, we did not observe any PD structural alterations or differences in PD frequencies between the mutant and wild-type veins (Fig. 5, J–M; Table II; Supplemental Figs. S2 and S4). Therefore, although we cannot exclude the possibility that a visually undetectable defect limits PD trafficking, these data suggest that the carbohydrate accumulation phenotype of *tdy2* mutants is not due to PD ultrastructural perturbations. Rather, the collective data suggest that *Tdy2* affects PD trafficking of Suc through the CC-SE interface.

tdy2 Mutants Have Normal Stomatal Patterning and Callose Deposition in Sieve Plates and in Response to Wounding

Since *Tdy2* encodes a callose synthase, we examined the *tdy2* mutant for other potential defects consistent with the predicted gene function. Recent research has uncovered a number of roles for callose synthases in epidermal patterning, callose synthesis in sieve plates, and callose deposition in response to wounding. A mutation in the Arabidopsis callose synthase *AtGSL8* gene was found to disrupt stomatal spacing in the epidermis of the leaf (Guseman et al., 2010). To test for a role of *Tdy2* in epidermal patterning, we inspected epidermal impressions of *tdy2* mutant and wild-type leaves. Both *tdy2* mutant and wild-type leaves displayed the stereotypical linear cell files of stomata, epidermal pavement cells, and trichomes. No changes in stomatal spacing, cell shape, or epidermal patterning were observed (Fig. 6).

Other recent research reported that the *AtGSL7* gene functioned to synthesize callose in the phloem sieve plates (Barratt et al., 2011; Xie et al., 2011). To examine callose deposition at sieve plates and in response to wounding, we performed aniline blue staining. Aniline blue is a fluorescent dye that binds callose and emits a bright blue/white light under UV illumination (Ruzin, 1999). Wild-type and *tdy2* mutant leaves displayed similar aniline blue-positive staining of sieve plates and punctate staining of callose deposits at PD after wounding (Fig. 7). Therefore, these data suggest that *Tdy2* function is not required for wound callose synthesis, callose deposition at the sieve plate, or cell

Table II. *Frequency of PD per cellular interface in the veins of wild-type and tdy2 yellow leaf tissues*

The values represent means ± SD. No statistical differences were observed between wild-type and *tdy2* yellow leaf tissues as determined using Student's *t* test. In wild-type maize minor veins, two types of SEs are present: thin-walled SE (SE) and thick-walled SE (thSE; Evert et al., 1978). The SEs are connected to the CC and function in Suc phloem loading. The thSE are connected to VP cells and are postulated to be involved in the retrieval of Suc leaked to the apoplast (Fritz et al., 1983). The number of interfaces analyzed for wild-type and *tdy2* yellow tissues were 822 and 893 for the BS-VP interface, 680 and 853 for the VP-VP interface, 279 and 276 for the thSE-VP interface, and 396 and 548 for the thin-walled SE-CC interface, respectively. Differences in the number of cellular interfaces are due to the preponderance of some cell types (e.g. BS cells) relative to the scarcity of others (e.g. thSE; Evert et al., 1978).

Interface	No. of PD per Interface		No. of PD per Pit Field		No. of Pit Fields per Interface	
	Wild Type	*tdy2*	Wild Type	*tdy2*	Wild Type	*tdy2*
BS-VP	3.0 ± 0.2	2.8 ± 0.3	6.1 ± 0.1	6.2 ± 0.8	0.49 ± 0.05	0.45 ± 0.08
VP-VP	2.0 ± 0.3	1.8 ± 0.4	5.2 ± 0.2	4.8 ± 1.3	0.38 ± 0.04	0.38 ± 0.14
thSE-VP	0.40 ± 0.24	0.34 ± 0.13	1.8 ± 0.4	2.5 ± 1.2	0.21 ± 0.08	0.14 ± 0.04
SE-CC	0.25 ± 0.10	0.27 ± 0.06	2.4 ± 0.3	2.8 ± 0.9	0.10 ± 0.04	0.10 ± 0.02

wall formation in nonvascular cell types (Baker and Braun, 2008).

DISCUSSION

Here, we identified and characterized the maize *Tdy2* gene and showed that the *tdy2* mutation disrupts the functional development of the phloem and thereby leads to improper symplastic trafficking between the CC and SE. Multiple lines of evidence support this thesis: (1) TEM ultrastructural studies demonstrated alterations in phloem and xylem cells; (2) in developing leaves, *Tdy2* displayed the highest expression in young veins; (3) *tdy2* mutant yellow leaf tissues hyperaccumulated soluble sugars and starch; and (4) *tdy2* yellow leaf tissues failed to export labeled Suc or CF to the translocation stream, although if the tracer entered the phloem in normal-appearing *tdy2* green leaf tissue, it moved unobstructed long distance through the phloem SE. In particular, the high frequency and large size of the oil droplets in the CC of the *tdy2* yellow leaf tissues suggest that Suc uptake from the apoplast into these cells is occurring normally. In agreement with this hypothesis, antisense inhibition of the SUT that mediates apoplastic phloem loading in potato leaves reduced photoassimilate export and resulted in the accumulation of some of the excess fixed carbon as oil droplets in phloem parenchyma cells (Schulz et al., 1998). Furthermore, our data from the radiolabeled and CF dye tracer assays with *tdy2* leaves showed that the excess carbon accumulation did not result from a long-distance transport defect in the SE. Thus, the presence of the oil droplets in the *tdy2* CC supports the hypothesis of restricted symplastic transport between the CC and SE. Indeed, a severe reduction of the CC-SE PD size-exclusion limit (SEL) is a possible explanation of the failure of ^{14}C-labeled Suc and CF to enter into the phloem SE in *tdy2* yellow leaf regions. Based on *Tdy2* expression, the blockage to Suc movement through the CC-SE PD in *tdy2* mutant yellow leaf tissues may be an indirect consequence of an early defect in vein development.

The combination of carbohydrate hyperaccumulation, CC-SE symplastic trafficking defects, vascular differentiation defects, and gene identity suggest a previously unknown role for the callose synthase encoded by *Tdy2* in vascular development. Based on phylogenetic analyses, the closest related sequences in Arabidopsis to the maize TDY2 protein are AtGSL3, AtGSL6, AtGSL9, and AtGSL12. Arabidopsis mutants resulting from T-DNA insertions into these genes do not condition an observable phenotype; thus, their functions remain largely unknown (Enns et al., 2005; Chen and Kim, 2009; Vatén et al., 2011). However, AtGSL12 was recently shown to control callose deposition at PD during root development (Vatén et al., 2011). Loss-of-function mutants had no apparent phenotype, but gain-of-function mutations under the control of a stele-specific

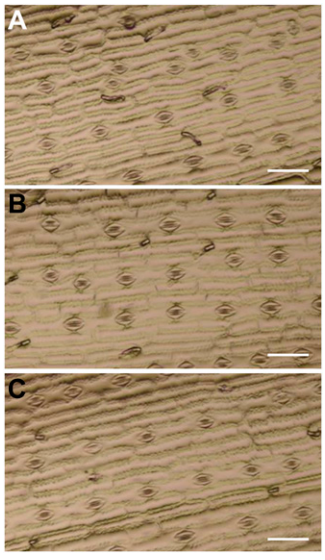

Figure 6. Epidermal cell patterning is normal in *tdy2-R* mutant leaves. Nail-polish impressions of the leaf epidermis showing normal spacing, cell shape, and stomatal cell files are shown. A, The wild type. B, *tdy2-R* green leaf region. C, *tdy2-R* yellow leaf region. Bars = 100 μm. [See online article for color version of this figure.]

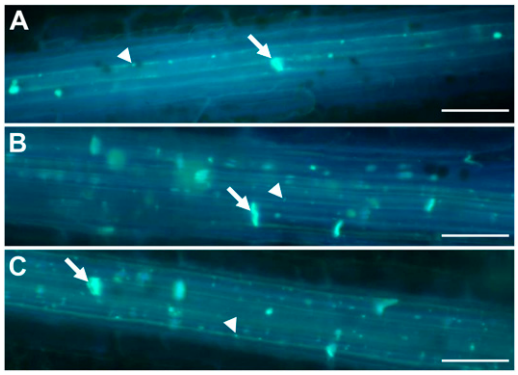

Figure 7. Aniline blue staining of callose in wounded leaves. A, The wild type. B, *tdy2-R* green leaf region. C, *tdy2-R* yellow leaf region. Images show callose staining using aniline blue 10 min after removal of the epidermal surface. The callose is visualized as bright blue fluorescence. White arrows identify callose at the sieve plates, and white arrowheads identify callose deposition at PD along the SE cell wall. Bars = 50 μm. [See online article for color version of this figure.]

promoter caused a transient increase in callose present at the neck of PD, reduced symplastic trafficking of macromolecules, and stunted root growth. Interestingly, defects in differentiation were observed in both the phloem and xylem tissues in the roots of these gain-of-function mutants. No phenotypes were reported in mutant leaves. These data are consistent with our hypothesized role for *Tdy2* functioning in vascular maturation and ultimately impacting symplastic transport through the CC-SE PD.

Because *Tdy2* is expressed broadly in all tissues examined, we sought to determine if it had additional roles similar to other callose synthases. *AtGSL7* is an Arabidopsis callose synthase evolutionarily more distantly related to *Tdy2* and is required for callose deposition during wound response and at the sieve plates in the mature phloem of Arabidopsis (Barratt et al., 2011; Xie et al., 2011). However, *tdy2* mutants were indistinguishable from wild-type plants in terms of callose accumulation at the sieve plates and wound callose deposition in the phloem, suggesting that *AtGSL7* and *Tdy2* have distinct functions. Lesions in a more closely related Arabidopsis callose synthase, *GSL8*, cause developmental defects in a number of different cell types throughout the plant (Chen et al., 2009; Guseman et al., 2010). The *gsl8* mutant vegetative phenotypes are likely due to defects in the new cell wall that forms between two daughter cells during cytokinesis and to the increased cell-to-cell trafficking of cell differentiation factors. However, significant differences are observed between *tdy2* and *gsl8* mutants. For example, we did not observe any stomatal or epidermal pavement cell-patterning defects, cell wall stubs, or multinucleate cells indicative of cytokinesis defects in the epidermis, suggesting that *Tdy2* function is not required for epidermal patterning. Furthermore, the PD in Arabidopsis *gsl8* mutants have been reported to show an increased SEL, as shown by a transient expression assay that bombarded DNA encoding differently sized GFP fusion proteins into the epidermal cells (Guseman et al., 2010). However, because the phloem is inaccessibly embedded within the center of the maize leaf, we could not perform a similar test for altered PD SEL in *tdy2* mutants. Nonetheless, the large oil droplets present in *tdy2* CCs indicate a reduced, rather than increased, SEL at the CC-SE interface, suggesting that the callose synthase encoded by *Tdy2* indirectly impacts symplastic trafficking through the CC-SE PD via its role in vascular development. As xylem cell differentiation defects also occur in *tdy2* mutants, one possibility that warrants further investigation is that xylem vessel differentiation also requires symplastic trafficking.

PD are dynamic cellular structures responsive to numerous inputs, such as genetic mutations affecting PD aperture or numbers (Benitez-Alfonso et al., 2009; Stonebloom et al., 2009; Burch-Smith and Zambryski, 2010), pathogen attack (Wolf et al., 1989; Ding et al., 1992), and the developmental stage of the tissue (Oparka et al., 1999; Crawford and Zambryski, 2001; Itaya et al., 2002; for review, see Burch-Smith et al., 2011; Ueki and Citovsky, 2011). In *tdy2* yellow leaf tissues, multiple lines of physiological and cytological evidence support the blockage in Suc movement occurring at the CC-SE PD; however, extensive ultrastructural studies failed to find any alterations to PD or changes in their frequency. Consistent with these results, previous investigations have observed that physical changes in PD are not always apparent with changes in the selectivity of, or solute transport through, PD. For example, expressing the movement protein of the *Tobacco mosaic virus* in plant cells increased the cell-to-cell trafficking of fluorescently labeled dextrans and carbohydrates but did not change the appearance of the PD by TEM (Wolf et al., 1989). Indeed, most viral movement proteins do not induce morphologically observable changes in PD by altering their SEL (Ueki and Citovsky, 2011). Hence, changes in PD trafficking do not require detectable alterations to PD structure, in agreement with our *tdy2* PD ultrastructural results.

The *tdy2* yellow and green leaf variegation phenotype requires high light, and once formed, these regions are developmentally stable for the lifetime of the leaf (Baker and Braun, 2008). Together with the *tdy2* vein differentiation and CC-SE PD trafficking defects described here, these data indicate that as a region of leaf tissue is developing, the capacity for symplastic transport through the CC-SE PD is sensitive to the environment. Furthermore, in addition to symplastic transport limitations, structural constraints, such as PD architecture and density, are relatively immutable once the tissue is mature (Amiard et al., 2005; Adams et al., 2007). These findings indicate that the local environment present during the early stages of leaf growth can determine the overall net export ability, irrespective of the future photosynthetic capacity of that leaf. In addition,

our work demonstrates that perturbations to symplastic transport between the CC and SE impact phloem export from leaves.

MATERIALS AND METHODS

Genetic Stocks

The *tdy2-R* and *tdy2-t112* alleles were isolated from ethyl methanesulfonate (EMS)-mutagenized F2 populations. Five *Mu* alleles were recovered from a directed transposon-tagging screen. The F1 plants were crossed to *Mu killer* stocks (Slotkin et al., 2003, 2005), and the alleles were backcrossed into the maize (*Zea mays*) inbred line B73 at least three times prior to analysis. PCR using *Mu*- and gene-specific primers was used to genotype *tdy2-Mu* mutant plants (Supplemental Table S1). Plants were grown as reported previously (Braun et al., 2006; Huang et al., 2009; Slewinski and Braun, 2010b). The *tdy2-R* mutant was used for the analyses.

Transport Studies

[U-^{14}C]Suc and CFDA labeling studies were performed as described previously (Ma et al., 2009; Slewinski et al., 2009). Six independent samples were analyzed for each of the [^{14}C]Suc and CF transport assays.

Gene Cloning and Phylogenetic Analysis

We performed a modified *Mu*-TAIL-PCR to clone the *Tdy2* flanking genomic DNA (Supplemental Materials and Methods S1). Transposon insertions in the additional *Mu* alleles were identified by PCR (Table I). Exons and UTRs were sequenced from the EMS alleles and compared with the sequences of their respective progenitors. For phylogenetic analysis, full-length protein sequences were retrieved for Arabidopsis, rice (*Oryza sativa*), sorghum (*Sorghum bicolor*), and maize (*Zea mays* 'B73') from www.phytozome.org. Sequences were aligned using MUSCLE, and neighbor-joining phylogenetic analysis was performed using PhyML with 1,000 repetitions and visualized using TreeDyn (Dereeper et al., 2008).

Gene Expression Analysis and ZmPIN1a Visualization

RT-PCR was performed with *Tdy2*-specific primers (Supplemental Table S1) on complementary DNA synthesized from RNA extracted from immature and mature leaves, roots, stems, tassels, and ears harvested from B73 plants, as described (Slewinski et al., 2009; Phillips et al., 2011). A unique genomic DNA fragment of *Tdy2* was PCR amplified using the primers *Tdy2* 3′ UTR B and CAL 7A (Supplemental Table S1) and TA cloned into pGEM T-Easy vector (Promega) for RNA probe synthesis. Immature leaf material from 6-week-old B73 plants was used for RNA in situ hybridization, performed as described (Jackson et al., 1994; Ma et al., 2009). Plants carrying the ZmPIN1a-YFP transgene (Gallavotti et al., 2008) were grown under similar conditions and were at the same developmental stage as plants used for the RNA in situ hybridizations. Free-hand cross-sections of immature leaf material were visualized under the same conditions described for the CF experiments.

Microscopy

Epidermal nail-polish impressions (Reynolds et al., 1998), callose and starch staining (Braun et al., 2006; Baker and Braun, 2008; Slewinski and Braun, 2010b), and TEM (Ma et al., 2008) were performed as described. For TEM, four minor veins (three small, one intermediate) that function in Suc phloem loading were harvested from a fully expanded adult leaf and examined in serial sections until a total of 100 individual vascular bundle sections were examined per leaf sample ($n = 3$, corresponding to 12 minor veins) for wild-type and *tdy2* yellow leaf tissues, respectively. The total number of PD was counted for each relevant cellular interface and then averaged relative to the total number of the respective interface type.

The sequence described in this paper has been deposited in GenBank under accession number JQ361049.

Supplemental Data

The following materials are available in the online version of this article.

Supplemental Figure S1. Molecular analysis of the *tdy2-m165* allele.

Supplemental Figure S2. Vein ultrastructure of *tdy2* green leaf tissue.

Supplemental Figure S3. Disrupted *tdy2* xylem elements contain starch.

Supplemental Figure S4. Ultrastructure of wild-type and *tdy2* yellow leaf tissue.

Supplemental Table S1. List of primers used.

Supplemental Materials and Methods S1.

ACKNOWLEDGMENTS

We thank two anonymous reviewers, as well as Andre Jagendorf, Cankui Zhang, Robert Turgeon, and Paula McSteen, for their helpful comments on the manuscript.

Received June 22, 2012; accepted August 28, 2012; published August 29, 2012.

LITERATURE CITED

Adams WW III, Watson AM, Mueh KE, Amiard V, Turgeon R, Ebbert V, Logan BA, Combs AF, Demmig-Adams B (2007) Photosynthetic acclimation in the context of structural constraints to carbon export from leaves. Photosynth Res **94:** 455–466

Ainsworth EA, Bush DR (2011) Carbohydrate export from the leaf: a highly regulated process and target to enhance photosynthesis and productivity. Plant Physiol **155:** 64–69

Amiard V, Mueh KE, Demmig-Adams B, Ebbert V, Turgeon R, Adams WW III (2005) Anatomical and photosynthetic acclimation to the light environment in species with differing mechanisms of phloem loading. Proc Natl Acad Sci USA **102:** 12968–12973

Ayre BG (2011) Membrane-transport systems for sucrose in relation to whole-plant carbon partitioning. Mol Plant **4:** 377–394

Baker RF, Braun DM (2007) *tie-dyed1* functions non-cell autonomously to control carbohydrate accumulation in maize leaves. Plant Physiol **144:** 867–878

Baker RF, Braun DM (2008) *tie-dyed2* functions with *tie-dyed1* to promote carbohydrate export from maize leaves. Plant Physiol **146:** 1085–1097

Baker RF, Leach KA, Braun DM (2012) SWEET as sugar: new sucrose efluxers in plants. Mol Plant **5:** 766–768

Barratt DHP, Kölling K, Graf A, Pike M, Calder G, Findlay K, Zeeman SC, Smith AM (2011) Callose synthase GSL7 is necessary for normal phloem transport and inflorescence growth in Arabidopsis. Plant Physiol **155:** 328–341

Benitez-Alfonso Y, Cilia M, San Roman A, Thomas C, Maule A, Hearn S, Jackson D (2009) Control of Arabidopsis meristem development by thioredoxin-dependent regulation of intercellular transport. Proc Natl Acad Sci USA **106:** 3615–3620

Blauth SL, Yao Y, Klucinec JD, Shannon JC, Thompson DB, Guilitinan MJ (2001) Identification of *Mutator* insertional mutants of starch-branching enzyme 2a in corn. Plant Physiol **125:** 1396–1405

Botha CEJ, Aoki N, Scofield GN, Liu L, Furbank RT, White RG (2008) A xylem sap retrieval pathway in rice leaf blades: evidence of a role for endocytosis? J Exp Bot **59:** 2945–2954

Botha CEJ, Cross RHM, van Bel AJE, Peter CI (2000) Phloem loading in the sucrose-export-defective (SXD-1) mutant maize is limited by callose deposition at plasmodesmata in bundle sheath-vascular parenchyma interface. Protoplasma **214:** 65–72

Braun DM (2012) SWEET! The pathway is complete. Science **335:** 173–174

Braun DM, Ma Y, Inada N, Muszynski MG, Baker RF (2006) *tie-dyed1* regulates carbohydrate accumulation in maize leaves. Plant Physiol **142:** 1511–1522

Braun DM, Slewinski TL (2009) Genetic control of carbon partitioning in grasses: roles of *sucrose transporters* and *tie-dyed* loci in phloem loading. Plant Physiol **149:** 71–81

Burch-Smith TM, Stonebloom S, Xu M, Zambryski PC (2011) Plasmodesmata during development: re-examination of the importance of

primary, secondary, and branched plasmodesmata structure versus function. Protoplasma **248:** 61–74

Burch-Smith TM, Zambryski PC (2010) Loss of INCREASED SIZE EXCLUSION LIMIT (ISE)1 or ISE2 increases the formation of secondary plasmodesmata. Curr Biol **20:** 989–993

Bürkle L, Hibberd JM, Quick WP, Kühn C, Hirner B, Frommer WB (1998) The H^+-sucrose cotransporter NtSUT1 is essential for sugar export from tobacco leaves. Plant Physiol **118:** 59–68

Chen L-Q, Qu X-Q, Hou B-H, Sosso D, Osorio S, Fernie AR, Frommer WB (2012) Sucrose efflux mediated by SWEET proteins as a key step for phloem transport. Science **335:** 207–211

Chen XY, Kim J-Y (2009) Callose synthesis in higher plants. Plant Signal Behav **4:** 489–492

Chen X-Y, Liu L, Lee E, Han X, Rim Y, Chu H, Kim S-W, Sack F, Kim J-Y (2009) The Arabidopsis callose synthase gene *GSL8* is required for cytokinesis and cell patterning. Plant Physiol **150:** 105–113

Crawford KM, Zambryski PC (2001) Non-targeted and targeted protein movement through plasmodesmata in leaves in different developmental and physiological states. Plant Physiol **125:** 1802–1812

Dereeper A, Guignon V, Blanc G, Audic S, Buffet S, Chevenet F, Dufayard J-F, Guindon S, Lefort V, Lescot M, et al (2008) Phylogeny.fr: robust phylogenetic analysis for the non-specialist. Nucleic Acids Res **36:** W465–W469

Ding B, Haudenshield JS, Hull RJ, Wolf S, Beachy RN, Lucas WJ (1992) Secondary plasmodesmata are specific sites of localization of the tobacco mosaic virus movement protein in transgenic tobacco plants. Plant Cell **4:** 915–928

Dinges JR, Colleoni C, James MG, Myers AM (2003) Mutational analysis of the pullulanase-type debranching enzyme of maize indicates multiple functions in starch metabolism. Plant Cell **15:** 666–680

Enns LC, Kanaoka MM, Torii KU, Comai L, Okada K, Cleland RE (2005) Two callose synthases, GSL1 and GSL5, play an essential and redundant role in plant and pollen development and in fertility. Plant Mol Biol **58:** 333–349

Esau K (1943) Ontogeny of the vascular bundles in *Zea mays*. Hilgardia **15:** 327–368

Esau K (1977) Anatomy of Seed Plants, Ed 2. John Wiley and Sons, New York

Evert RF, Eschrich W, Heyser W (1978) Leaf structure in relation to solute transport and phloem loading in *Zea mays* L. Planta **138:** 279–294

Fritz E, Evert RF, Heyser W (1983) Microautoradiographic studies of phloem loading and transport in the leaf of *Zea mays* L. Planta **159:** 193–206

Fritz E, Evert RF, Nasse H (1989) Loading and transport of assimilates in different maize leaf bundles: digital image analysis of ^{14}C microautoradiographs. Planta **178:** 1–9

Gallavotti A, Yang Y, Schmidt RJ, Jackson D (2008) The relationship between auxin transport and maize branching. Plant Physiol **147:** 1913–1923

Gottwald JR, Krysan PJ, Young JC, Evert RF, Sussman MR (2000) Genetic evidence for the *in planta* role of phloem-specific plasma membrane sucrose transporters. Proc Natl Acad Sci USA **97:** 13979–13984

Guseman JM, Lee JS, Bogenschutz NL, Peterson KM, Virata RE, Xie B, Kanaoka MM, Hong Z, Torii KU (2010) Dysregulation of cell-to-cell connectivity and stomatal patterning by loss-of-function mutation in *Arabidopsis chorus* (*glucan synthase-like 8*). Development **137:** 1731–1741

Hackel A, Schauer N, Carrari F, Fernie AR, Grimm B, Kühn C (2006) Sucrose transporter LeSUT1 and LeSUT2 inhibition affects tomato fruit development in different ways. Plant J **45:** 180–192

Huang M, Slewinski TL, Baker RF, Janick-Buckner D, Buckner B, Johal GS, Braun DM (2009) Camouflage patterning in maize leaves results from a defect in porphobilinogen deaminase. Mol Plant **2:** 773–789

Itaya A, Ma F, Qi Y, Matsuda Y, Zhu Y, Liang G, Ding B (2002) Plasmodesma-mediated selective protein traffic between "symplasmically isolated" cells probed by a viral movement protein. Plant Cell **14:** 2071–2083

Jackson D, Veit B, Hake S (1994) Expression of maize KNOTTED1 related homeobox genes in the shoot apical meristem predicts patterns of morphogenesis in the vegetative shoot. Development **120:** 405–413

Jiao Y, Wickett NJ, Ayyampalayam S, Chanderbali AS, Landherr L, Ralph PE, Tomsho LP, Hu Y, Liang H, Soltis PS, et al (2011) Ancestral polyploidy in seed plants and angiosperms. Nature **473:** 97–100

Kühn C, Franceschi VR, Schulz A, Lemoine R, Frommer WB (1997) Macromolecular trafficking indicated by localization and turnover of sucrose transporters in enucleate sieve elements. Science **275:** 1298–1300

Kühn C, Grof C (2010) Sucrose transporters of higher plants. Curr Opin Plant Biol **13:** 288–298

Lalonde S, Tegeder M, Throne-Holst M, Frommer W, Patrick J (2003) Phloem loading and unloading of sugars and amino acids. Plant Cell Environ **26:** 37–56

Lalonde S, Wipf D, Frommer WB (2004) Transport mechanisms for organic forms of carbon and nitrogen between source and sink. Annu Rev Plant Biol **55:** 341–372

Lersten NR, Czlapinski AR, Curtis JD, Freckmann R, Horner HT (2006) Oil bodies in leaf mesophyll cells of angiosperms: overview and a selected survey. Am J Bot **93:** 1731–1739

Lunn JE, Furbank RT (1999) Tansley Review No. 105. Sucrose biosynthesis in C_4 plants. New Phytol **143:** 221–237

Ma Y, Baker RF, Magallanes-Lundback M, DellaPenna D, Braun DM (2008) *tie-dyed1* and *sucrose export defective1* act independently to promote carbohydrate export from maize leaves. Planta **227:** 527–538

Ma Y, Slewinski TL, Baker RF, Braun DM (2009) *Tie-dyed1* encodes a novel, phloem-expressed transmembrane protein that functions in carbohydrate partitioning. Plant Physiol **149:** 181–194

Oparka KJ, Roberts AG, Boevink P, Santa Cruz S, Roberts I, Pradel KS, Imlau A, Kotlizky G, Sauer N, Epel B (1999) Simple, but not branched, plasmodesmata allow the nonspecific trafficking of proteins in developing tobacco leaves. Cell **97:** 743–754

Phillips KA, Skirpan AL, Liu X, Christensen A, Slewinski TL, Hudson C, Barazesh S, Cohen JD, Malcomber S, McSteen P (2011) *vanishing tassel2* encodes a grass-specific tryptophan aminotransferase required for vegetative and reproductive development in maize. Plant Cell **23:** 550–566

Provencher LM, Miao L, Sinha N, Lucas WJ (2001) *Sucrose export defective1* encodes a novel protein implicated in chloroplast-to-nucleus signaling. Plant Cell **13:** 1127–1141

Reynolds JO, Eisses JF, Sylvester AW (1998) Balancing division and expansion during maize leaf morphogenesis: analysis of the mutant, warty-1. Development **125:** 259–268

Riesmeier JW, Willmitzer L, Frommer WB (1994) Evidence for an essential role of the sucrose transporter in phloem loading and assimilate partitioning. EMBO J **13:** 1–7

Roberts AG, Oparka KJ (2003) Plasmodesmata and the control of symplastic transport. Plant Cell Environ **26:** 103–124

Russell SH, Evert RF (1985) Leaf vasculature in *Zea mays* L. Planta **164:** 448–458

Russin WA, Evert RF, Vanderveer PJ, Sharkey TD, Briggs SP (1996) Modification of a specific class of plasmodesmata and loss of sucrose export ability in the *sucrose export defective1* maize mutant. Plant Cell **8:** 645–658

Ruzin S (1999) Plant Microtechnique and Microscopy. Oxford University Press, New York

Sattler SE, Cahoon EB, Coughlan SJ, DellaPenna D (2003) Characterization of tocopherol cyclases from higher plants and cyanobacteria: evolutionary implications for tocopherol synthesis and function. Plant Physiol **132:** 2184–2195

Sauer N (2007) Molecular physiology of higher plant sucrose transporters. FEBS Lett **581:** 2309–2317

Schulz A, Kühn C, Riesmeier JW, Frommer WB (1998) Ultrastructural effects in potato leaves due to antisense-inhibition of the sucrose transporter indicate an apoplasmic mode of phloem loading. Planta **206:** 533–543

Singer T, Burke E (2003) High-throughput TAIL-PCR as a tool to identify DNA flanking insertions. Methods Mol Biol **236:** 241–271

Slewinski TL, Braun DM (2010a) Current perspectives on the regulation of whole-plant carbohydrate partitioning. Plant Sci **178:** 341–349

Slewinski TL, Braun DM (2010b) The *psychedelic* genes of maize redundantly promote carbohydrate export from leaves. Genetics **185:** 221–232

Slewinski TL, Garg A, Johal GS, Braun DM (2010) Maize SUT1 functions in phloem loading. Plant Signal Behav **5:** 687–690

Slewinski TL, Ma Y, Baker RF, Huang M, Meeley R, Braun DM (2008) Determining the role of *Tie-dyed1* in starch metabolism: epistasis analysis with a maize ADP-glucose pyrophosphorylase mutant lacking leaf starch. J Hered **99:** 661–666

Slewinski TL, Meeley R, Braun DM (2009) *Sucrose transporter1* functions in phloem loading in maize leaves. J Exp Bot **60:** 881–892

Slotkin RK, Freeling M, Lisch D (2003) *Mu killer* causes the heritable inactivation of the *Mutator* family of transposable elements in Zea mays. Genetics **165:** 781–797

Slotkin RK, Freeling M, Lisch D (2005) Heritable transposon silencing initiated by a naturally occurring transposon inverted duplication. Nat Genet **37:** 641–644

Srivastava AC, Ganesan S, Ismail IO, Ayre BG (2008) Functional characterization of the *Arabidopsis thaliana* AtSUC2 Suc/H^+ symporter by tissue-specific complementation reveals an essential role in phloem loading but not in long-distance transport. Plant Physiol **147:** 200–211

Stonebloom S, Burch-Smith T, Kim I, Meinke D, Mindrinos M, Zambryski PC (2009) Loss of the plant DEAD-box protein ISE1 leads to defective mitochondria and increased cell-to-cell transport via plasmodesmata. Proc Natl Acad Sci USA **106:** 17229–17234

Turner S, Gallois P, Brown D (2007) Tracheary element differentiation. Annu Rev Plant Biol **58:** 407–433

Ueki S, Citovsky V (2011) To gate, or not to gate: regulatory mechanisms for intercellular protein transport and virus movement in plants. Mol Plant **4:** 782–793

Vatén A, Dettmer J, Wu S, Stierhof Y-D, Miyashima S, Yadav SR, Roberts CJ, Campilho A, Bulone V, Lichtenberger R, et al (2011) Callose biosynthesis regulates symplastic trafficking during root development. Dev Cell **21:** 1144–1155

Verma DPS, Hong Z (2001) Plant callose synthase complexes. Plant Mol Biol **47:** 693–701

Wenzel CL, Schuetz M, Yu Q, Mattsson J (2007) Dynamics of MONOPTEROS and PIN-FORMED1 expression during leaf vein pattern formation in *Arabidopsis thaliana*. Plant J **49:** 387–398

Wolf S, Deom CM, Beachy RN, Lucas WJ (1989) Movement protein of tobacco mosaic virus modifies plasmodesmatal size exclusion limit. Science **246:** 377–379

Wright K, Oparka KJ (1996) The fluorescent probe HPTS as a phloem-mobile, symplastic tracer: an evaluation using confocal laser scanning microscopy. J Exp Bot **47:** 439–445

Xie B, Wang X, Zhu M, Zhang Z, Hong Z (2011) *CalS7* encodes a callose synthase responsible for callose deposition in the phloem. Plant J **65:** 1–14

Zhang B, Tolstikov V, Turnbull C, Hicks LM, Fiehn O (2010) Divergent metabolome and proteome suggest functional independence of dual phloem transport systems in cucurbits. Proc Natl Acad Sci USA **107:** 13532–13537